

This article was downloaded by:

On: 23 January 2011

Access details: *Access Details: Free Access*

Publisher *Taylor & Francis*

Informa Ltd Registered in England and Wales Registered Number: 1072954 Registered office: Mortimer House, 37-41 Mortimer Street, London W1T 3JH, UK



Journal of Coordination Chemistry

Publication details, including instructions for authors and subscription information:

<http://www.informaworld.com/smpp/title~content=t713455674>

Synthesis and crystal structures of Cd(II), Ni(II), and Mn(II) complexes of 1H-benzotriazole-1-acetic acid

Zebao Zheng^a; Rentao Wu^a; Jikun Li^b; Yinfeng Han^a; Jingrong Lu^a

^a Department of Chemistry and Environmental Science, Taishan University, Taian, P.R. China ^b

Department of Materials and Chemical Engineering, Taishan University, Taian, P.R. China

First published on: 01 April 2010

To cite this Article Zheng, Zebao , Wu, Rentao , Li, Jikun , Han, Yinfeng and Lu, Jingrong(2010) 'Synthesis and crystal structures of Cd(II), Ni(II), and Mn(II) complexes of 1H-benzotriazole-1-acetic acid', *Journal of Coordination Chemistry*, 63: 7, 1118 – 1129, First published on: 01 April 2010 (iFirst)

To link to this Article: DOI: 10.1080/00958971003749706

URL: <http://dx.doi.org/10.1080/00958971003749706>

PLEASE SCROLL DOWN FOR ARTICLE

Full terms and conditions of use: <http://www.informaworld.com/terms-and-conditions-of-access.pdf>

This article may be used for research, teaching and private study purposes. Any substantial or systematic reproduction, re-distribution, re-selling, loan or sub-licensing, systematic supply or distribution in any form to anyone is expressly forbidden.

The publisher does not give any warranty express or implied or make any representation that the contents will be complete or accurate or up to date. The accuracy of any instructions, formulae and drug doses should be independently verified with primary sources. The publisher shall not be liable for any loss, actions, claims, proceedings, demand or costs or damages whatsoever or howsoever caused arising directly or indirectly in connection with or arising out of the use of this material.

Synthesis and crystal structures of Cd(II), Ni(II), and Mn(II) complexes of 1H-benzotriazole-1-acetic acid

ZEBAO ZHENG*[†], RENTAO WU[†], JIKUN LI[‡],
YINFENG HAN[†] and JINGRONG LU[†]

[†]Department of Chemistry and Environmental Science, Taishan University,
Taian, Shandong, 271021, P.R. China

[‡]Department of Materials and Chemical Engineering, Taishan University,
Taian, Shandong, 271021, P.R. China

(Received 16 August 2009; in final form 2 December 2009)

Three new complexes: $[\text{Cd}(\text{btaa})(\text{bipy})(\text{CH}_3\text{COO}) \cdot \text{H}_2\text{O}]_n$ (**1**), $[\text{Ni}(\text{btaa})_2(\text{H}_2\text{O})_4 \cdot 6\text{H}_2\text{O}]_n$ (**2**), and $[\text{Mn}(\text{btaa})_2(\text{H}_2\text{O})_2]_n$ (**3**) (bipy = 2,2'-bipyridine, Hbtaa = 1H-benzotriazole-1-acetic acid) were prepared and characterized by IR, elemental analyses, thermogravimetric analyses, and single-crystal X-ray analyses. In **1**, cadmium ions are linked by btaa ligands into 1-D linear chains; the chains are extended into layers through C–H \cdots O hydrogen bonds and π – π stacking interactions. Complex **2** is a mononuclear structure, extended to a 3-D network through multiple intermolecular hydrogen bonds. In **3**, manganese is bridged by carboxylate groups of btaa in the *syn-skew* bidentate mode in two directions to form a 2-D grid-like framework with a (4, 4) topology. The solid-state fluorescence spectrum of **1** shows that the excitation peak is at 355 nm while the maximum emission peak is at 424 nm.

Keywords: Coordination compounds; Hydrogen bonds; 1H-benzotriazole-1-acetic acid; Fluorescent property

1. Introduction

Crystal engineering of coordination polymers has attracted attention because of their enormous variety of interesting structural topologies and potential applications as functional materials [1–5]. Hydrogen bonding and π – π stacking interactions greatly affect the structures of coordination polymers [6], linking low-dimensional entities into high-dimensional supramolecular networks [7].

As a ligand with multiple coordination sites, benzotriazole is a good linker in generation of metal–organic frameworks (MOFs) as it can bridge different metal centers to afford coordination polymers that exhibit structural diversity and facile accessibility of functionalized new magnetic materials [8–10]. Functional groups such as carboxylate, hydroxy, and pyridyl can be introduced in benzotriazole, increasing coordination possibilities [11–14]. Polycyclic aromatic chelating ligands such as 2,2'-bipyridine (2,2'-bipy) and 1,10-phenanthroline (1,10-phen) are often introduced

*Corresponding author. Email: zhengzebao@163.com

as auxiliary ligands to control the structure and dimensionality of the resulting coordination polymers [15, 16].

As a flexible ligand 1H-benzotriazole-1-acetic acid (Hbtaa) contains a carboxylate group and a triazole to construct MOFs. Hu *et al.* [17, 18] have made a systemic investigation on Ag(I) and Zn(II) frameworks based on Hbtaa. We have also been interested in metal–triazole systems and reported a series of K(I), Zn(II), Ni(II), Mn(II), and Cu(II) frameworks [19, 20]. As continuation of previous work, herein we report the preparation and crystal structures of three new coordination polymers: $[\text{Cd}(\text{btaa})(\text{bipy})(\text{CH}_3\text{COO}) \cdot \text{H}_2\text{O}]_n$ (**1**), $[\text{Ni}(\text{btaa})_2(\text{H}_2\text{O})_4 \cdot 6\text{H}_2\text{O}]_n$ (**2**), and $[\text{Mn}(\text{btaa})_2(\text{H}_2\text{O})_2]_n$ (**3**).

2. Experimental

2.1. Synthesis of $[\text{Cd}(\text{btaa})(\text{bipy})(\text{CH}_3\text{COO}) \cdot \text{H}_2\text{O}]_n$ (**1**)

1H-Benzotriazole-1-acetic acid was synthesized according to the literature [21]. All other reagents were commercially available and used as received.

A mixture of $\text{Cd}(\text{CH}_3\text{COO})_2 \cdot 2\text{H}_2\text{O}$ (0.267 g, 1 mmol), Hbtaa (0.177 g, 1 mmol), and 2,2'-bipy (0.164 g, 1 mmol) was dissolved in methanol (10 mL), and the pH of the solution was adjusted to 6–7 with 0.2 M aqueous NaOH and the solution was stirred for 3 h at room temperature. The solution was filtered and the filtrate was allowed to stand at room temperature. After slow evaporation over 3 weeks, colorless block single crystals were obtained. Yield: 52% based on Cd. Anal. Calcd for $\text{C}_{20}\text{H}_{19}\text{CdN}_5\text{O}_5$: C, 46.03; H, 3.67; N, 13.42. Found: C, 46.11; H, 3.58; N, 13.47. IR (KBr, cm^{-1}): 3421(s), 2910(m), 1603(s), 1567(m), 1398(s), 1320(m), 1210(m), 990(m), 758(s).

2.2. Synthesis of $[\text{Ni}(\text{btaa})_2(\text{H}_2\text{O})_4 \cdot 6\text{H}_2\text{O}]_n$ (**2**)

A mixture of $\text{Ni}(\text{CH}_3\text{COO})_2 \cdot 2\text{H}_2\text{O}$ (0.107 g, 0.5 mmol) and Hbtaa (0.177 g, 1 mmol) was dissolved in water (12 mL) and ethanol (3 mL) and the pH of the solution was adjusted to 6–7 with 0.2 M aqueous NaOH. The mixed solution was stirred for 30 min at room temperature and transferred to and sealed in a 25 mL Teflon-lined stainless-steel reactor, and then heated at 150°C for 72 h; upon cooling to room temperature, a colorless solution and a small amount of blue precipitate were obtained. The solution was filtered and the filtrate was allowed to stand at room temperature. After slow evaporation for over 3 days, blue block single crystals were obtained. Yield: 42% based on Ni. Anal. Calcd for $\text{C}_{16}\text{H}_{32}\text{NiN}_6\text{O}_{14}$: C, 32.50; H, 5.46; N, 14.21. Found: C, 32.44; H, 5.41; N, 14.28. IR (KBr, cm^{-1}): 3390(s), 2924(m), 1603(s), 1393(s), 1306(m), 1224(m), 1142(m), 743(s).

2.3. Synthesis of $[\text{Mn}(\text{btaa})_2(\text{H}_2\text{O})_2]_n$ (**3**)

Compound **3** was obtained using a procedure similar to that used for **2** except that $\text{Mn}(\text{CH}_3\text{COO})_2 \cdot 4\text{H}_2\text{O}$ (0.123 g, 0.5 mmol) was used instead of $\text{Ni}(\text{CH}_3\text{COO})_2 \cdot 2\text{H}_2\text{O}$. Light yellow block single crystals were obtained. Yield: 40% based on Mn. Anal. Calcd

for $C_{16}H_{16}MnN_6O_6$: C, 43.35; H, 3.64; N, 18.95. Found: C, 43.30; H, 3.71; N, 18.90. IR (KBr, cm^{-1}): 3308(s), 2927(m), 1608(s), 1444(s), 1317(m), 1265(m), 1106(m), 784(s).

2.4. X-ray crystallography

Suitable single crystals of **1**, **2**, and **3** were carefully selected under an optical microscope and glued to thin glass fibers. Diffraction data were collected with graphite-monochromated Mo-K α radiation ($\lambda = 0.71073 \text{ \AA}$) on a Bruker APEX-II area-detector. Intensities were collected by the ω - 2θ scan technique. The structures were solved by direct methods and refined with full-matrix least-squares (SHELXTL-97) [21]. Hydrogens were placed in calculated positions. The crystal data and experimental details of the structure determinations are listed in table 1. The selected bond lengths and angles are listed in tables 2–4.

2.5. Physical measurements

Elemental analyses (C, H, N) were determined on an Elementar Carlo EL elemental analyzer. Infrared (IR) spectroscopy on KBr pellets was performed on a Nexus 912 AO446 FT-IR spectrophotometer from 4000 to 400 cm^{-1} . Thermogravimetric analyses (TGA) were carried out on a Delta Series TA-SDTQ600 in nitrogen from room temperature to 600°C (heating rate = 10°C min^{-1}) using aluminum crucibles. Luminescence measurements were carried out in the solid state at room temperature with a Perkin-Elmer LS 55 spectrofluorimeter.

Table 1. Crystal, data collection and structure refinement parameters for **1**–**3**.

Complex	1	2	3
Chemical formula	$C_{20}H_{19}CdN_5O_5$	$C_{16}H_{32}NiN_6O_{14}$	$C_{16}H_{16}MnN_6O_6$
Formula weight	521.80	591.19	443.29
Crystal system	Triclinic	Triclinic	Monoclinic
Space group	$P\bar{1}$	$P\bar{1}$	$P 2(1)/c$
Unit cell dimensions (\AA , $^\circ$)			
<i>a</i>	8.209(6)	7.601(2)	16.244(3)
<i>b</i>	9.436(7)	9.028(2)	6.998(1)
<i>c</i>	14.158(1)	9.862(2)	7.968(2)
α	93.174(1)	109.080(3)	90
β	97.816(1)	97.045(4)	90.160(3)
γ	106.415(1)	96.402(4)	90
Volume (\AA^3), <i>Z</i>	1037.2(1), 2	626.4(2), 1	905.7(3), 2
Calculated density ($mg\ m^{-3}$)	1.671	1.567	1.625
<i>F</i> (000)	524	310	454
μ (mm^{-1})	1.096	0.854	0.779
Crystal size (mm^3)	$0.18 \times 0.16 \times 0.15$	$0.18 \times 0.16 \times 0.13$	$0.16 \times 0.12 \times 0.10$
θ range ($^\circ$)	2.26–25.05	2.22–25.05	2.56–25.04
Reflections collected	5498	3265	4796
Unique reflections	3642 ($R_{int} = 0.0135$)	2188 ($R_{int} = 0.0202$)	1600 ($R_{int} = 0.0652$)
Data/restraints/parameters	3642/0/280	2188/0/169	1600/0/134
Goodness-of-fit on F^2	1.094	1.047	1.011
Final <i>R</i> indices [$I > 2\sigma(I)$]	$R_1 = 0.0214$, $wR_2 = 0.0561$	$R_1 = 0.0390$, $wR_2 = 0.0935$	$R_1 = 0.0290$, $wR_2 = 0.0738$
<i>R</i> indices (all data)	$R_1 = 0.0225$, $wR_2 = 0.0567$	$R_1 = 0.0470$, $wR_2 = 0.0985$	$R_1 = 0.0319$, $wR_2 = 0.0761$
Largest difference in peak and hole ($e\ \text{\AA}^{-3}$)	0.297 and -0.453	0.480 and -0.469	0.462 and -0.346

Table 2. Selected bond lengths (Å) and angles (°) for **1**.

Cd(1)–O(3)	2.242(2)	Cd(1)–O(2)#1	2.416(2)
Cd(1)–N(4)	2.333(2)	Cd(1)–O(1)#1	2.464(2)
Cd(1)–N(5)	2.354(2)	Cd(1)–O(4)	2.638(2)
Cd(1)–N(3)	2.390(2)		
O(3)–Cd(1)–N(4)	156.93(7)	O(3)–Cd(1)–O(1)#1	82.87(7)
O(3)–Cd(1)–N(5)	93.18(7)	N(4)–Cd(1)–O(1)#1	110.45(7)
N(4)–Cd(1)–N(5)	69.84(7)	N(5)–Cd(1)–O(1)#1	86.27(6)
O(3)–Cd(1)–N(3)	91.28(7)	N(3)–Cd(1)–O(1)#1	126.33(7)
N(4)–Cd(1)–N(3)	95.14(7)	O(2)#1–Cd(1)–O(1)#1	53.00(6)
N(5)–Cd(1)–N(3)	147.40(6)	O(3)–Cd(1)–O(4)	52.02(6)
O(3)–Cd(1)–O(2)#1	113.66(7)	N(4)–Cd(1)–O(4)	108.28(6)
N(4)–Cd(1)–O(2)#1	89.18(7)	N(5)–Cd(1)–O(4)	81.41(6)
N(5)–Cd(1)–O(2)#1	124.47(6)	N(3)–Cd(1)–O(4)	76.09(6)
N(3)–Cd(1)–O(2)#1	82.41(6)	O(2)#1–Cd(1)–O(4)	153.23(7)
O(1)#1–Cd(1)–O(4)	131.98(6)		

Symmetry transformations used to generate equivalent atoms: #1: $x+1, y, z$.

Table 3. Selected bond lengths (Å) and angles (°) for **2**.

Ni(1)–O(4)	2.064(2)	Ni(1)–O(3)	2.080(2)
Ni(1)–N(1)	2.087(2)	Ni(1)–N(1)#1	2.087(2)
Ni(1)–O(3)#1	2.080(2)	Ni(1)–O(4)#1	2.064(2)
O(4)–Ni(1)–O(4)#1	180.00(13)	O(3)–Ni(1)–N(1)	91.64(8)
O(4)–Ni(1)–O(3)#1	90.75(8)	O(4)–Ni(1)–N(1)#1	90.88(8)
O(4)–Ni(1)–O(3)	89.25(8)	O(3)–Ni(1)–N(1)#1	88.36(8)
O(3)#1–Ni(1)–O(3)	180.00(10)	N(1)–Ni(1)–N(1)#1	180.00(8)
O(4)–Ni(1)–N(1)	89.12(8)	O(4)#1–Ni(1)–N(1)	90.88(8)

Symmetry transformations used to generate equivalent atoms: #1: $-x, -y, -z$.

Table 4. Selected bond lengths (Å) and angles (°) for **3**.

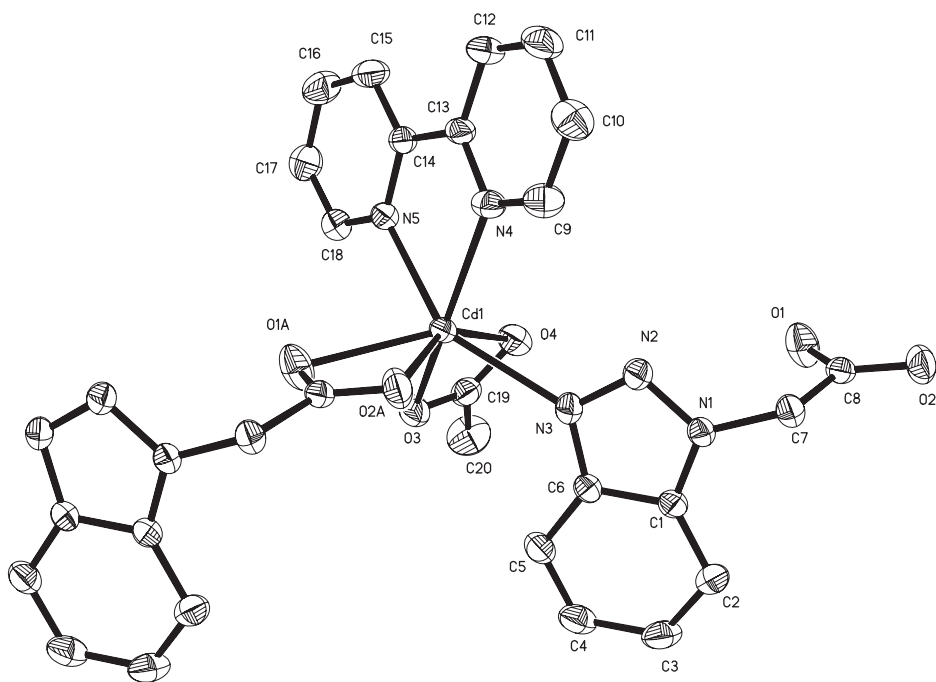
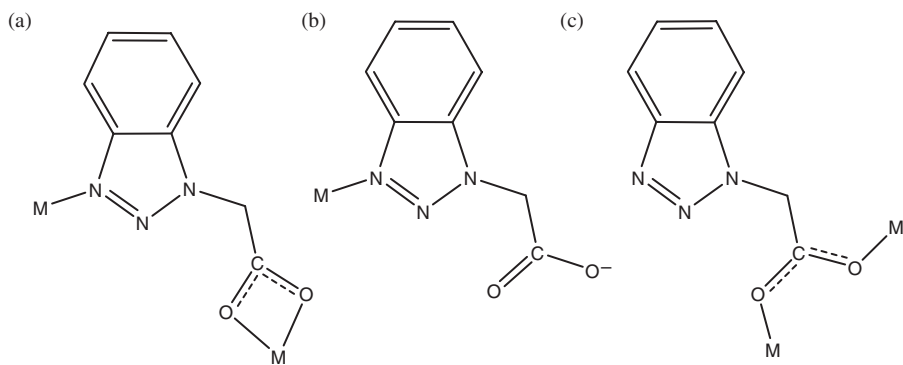
Mn(1)–O(2)#1	2.150(2)	Mn(1)–O(1)	2.173(2)
Mn(1)–O(3)	2.203(2)	Mn(1)–O(2)#2	2.150(2)
Mn(1)–O(1)#3	2.173(2)	Mn(1)–O(3)#3	2.203(2)
O(2)#1–Mn(1)–O(2)#2	180.0	O(1)–Mn(1)–O(3)	89.37(6)
O(2)#1–Mn(1)–O(1)#3	95.58(6)	O(1)–Mn(1)–O(3)#3	90.63(6)
O(2)#1–Mn(1)–O(1)	84.42(6)	O(3)–Mn(1)–O(3)#3	180.0
O(1)#3–Mn(1)–O(1)	180.0	O(2)#2–Mn(1)–O(3)	90.03(7)
O(2)#1–Mn(1)–O(3)	89.97(7)		

Symmetry transformations used to generate equivalent atoms: #1: $-x+2, y+1/2, -z+3/2$; #2: $x, -y+1/2, z-1/2$; #3: $-x+2, -y+1, -z+1$.

3. Results and discussion

3.1. Description of the crystal structure for $[Cd(btaa)(bipy)(CH_3COO) \cdot H_2O]_n$ (**1**)

The coordination environment of Cd(II) in **1** is shown in figure 1. Cd(II) is seven-coordinate with two oxygens from a btaa ligand, two μ_2 carboxyl oxygens of acetate, two nitrogens from one 2,2'-bipy ligand, and one nitrogen from a btaa ligand. The Cd–O distances are in the range 2.242(2) to 2.638(2) Å (table 2), the mean Cd–O bond distance [2.440(2) Å] is slightly longer than that of cadmium complex of 2-(1*H*-imidazole-1-yl)acetic acid [2.349(4) Å] [22], while Cd–N distances are in the range

Figure 1. ORTEP drawing (50% thermal) of **1**.

Scheme 1. The coordination modes of btaa.

2.333(2) to 2.390(2) Å, similar to those in the Cd(II) analogue with 2,2'-bipy ligands [23]. Cd(II) exhibits a distorted monocapped octahedral coordination geometry, in which the basal plane is formed by three nitrogens (N3, N4, and N5) and one oxygen (O3) with a mean deviation of 0.1205 Å from the least-squares plane, the corresponding axial positions are taken by two oxygens (O2A and O4) with an O2A–Cd1–O4 angle of 153.23(7)° and one carbonyl oxygen from btaa (O1A) occupies the capped position.

In **1**, btaa is chelate-tridentate [mode (a) in scheme 1] linking two adjacent Cd(II)s into linear chains (figure 2) running along the *c*-axis with the 2,2'-bipy attached at one side.

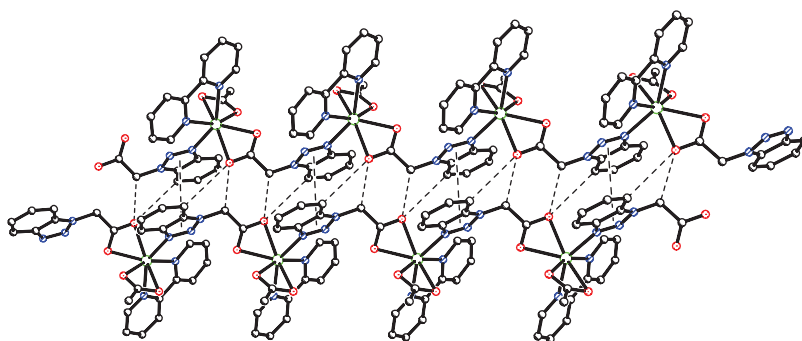


Figure 2. Perspective views of the 1-D double-chains in **1**; hydrogen bonds are shown as dashed lines. All hydrogens are omitted.

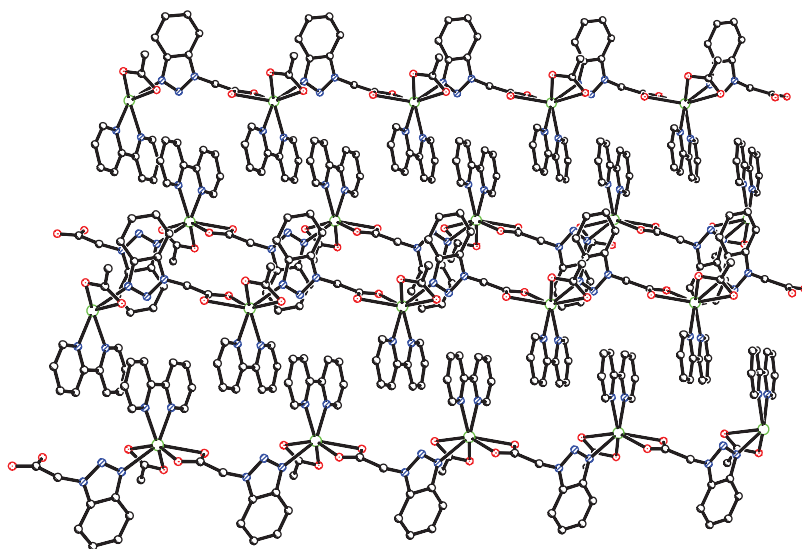
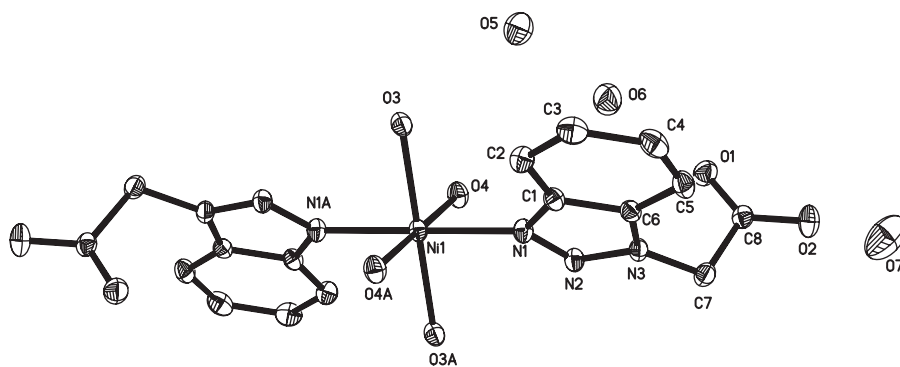
Two adjacent, centrosymmetrically related linear chains are assembled through interchain C–H \cdots O hydrogen bonds [C2 \cdots O2a, 3.440(1); C7 \cdots O2a, 3.448(1) Å; symmetry codes: a: ($-x, -y, z + 2$)] and π – π stacking interactions (offset π – π interactions between triazole rings with a face-to-face distance of 3.485 Å and offset angle of 22.18°) into a double-chain with the 2,2'-bipy ligands orientated at both sides. This arrangement is similar to the cadmium complex of thiophene-2,5-dicarboxylic acid and 2,2'-bipy [Cd(tdc)(2,2'-bipy)(H₂O)]_n [24]. The double-chains are extended into layers through offset aromatic π – π stacking interactions between 2,2'-bipy ligands (the face-to-face distance *ca* 3.528 Å and offset angle of 20.02°) (figure 3).

Lattice water behaves as the donor of two O–H \cdots O bonds (O5 \cdots O1A = 2.851 Å and O5 \cdots O4A = 2.797 Å, and the angles O5–H21 \cdots O1A = 163.84°, O5–H22 \cdots O4 = 161.24°; symmetry codes a: $-x + 1, -y + 1, -z + 1$) with two carboxylate oxygens from one acetate and one btaa ligand, coming from the same linear chain, stabilizing the chain structure.

3.2. Description of the crystal structure for [Ni(btaa)₂(H₂O)₄ · 6H₂O]_n (**2**)

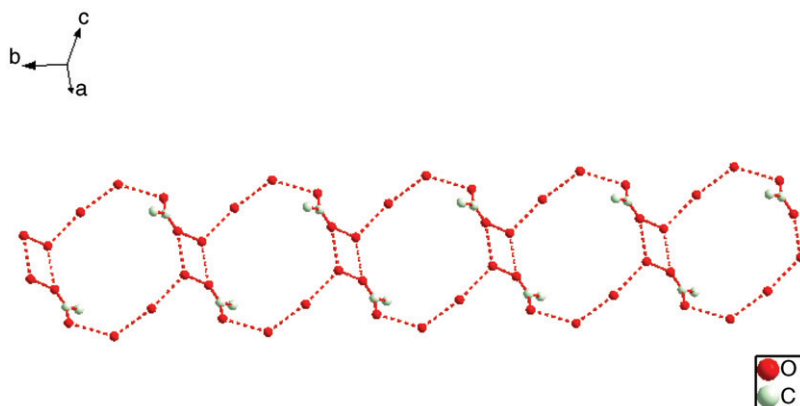
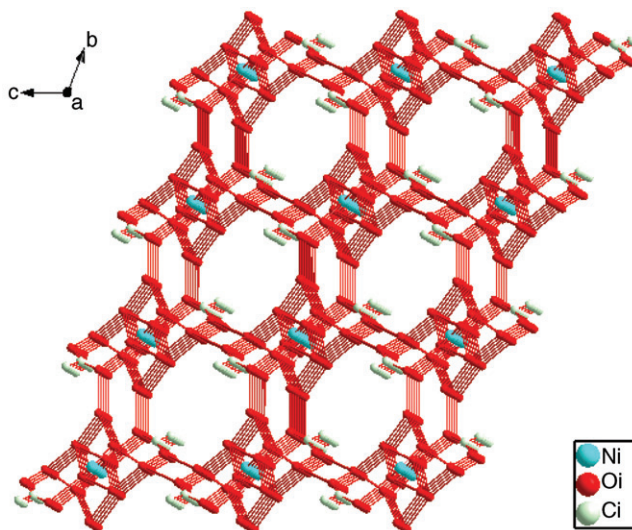
In this neutral mononuclear molecule, Ni(II) is located at the crystallographic inversion center. The octahedral coordination sphere is furnished by a pair of nitrogens from two btaa and four waters (see table 3 for detailed bond parameters). As shown in figure 4, although the ligand is deprotonated, only the triazole group is involved in metal coordination [mode (b) in scheme 1].

Multiple hydrogen-bonding interactions are observed in this structure (table 5). As illustrated in figure 5, the crystal-lattice waters and oxygens of carboxylate are interlinked by O–H \cdots O hydrogen bonds into 1-D tapes along the *b*-axis. The tapes consist of fused 4- and 12-membered rings, resulting in a water cluster notation as T4(2)12(2) according to Infantes' classification [25]. Additionally, these tapes are further connected with adjacent Ni(H₂O)₄ spheres through O–H \cdots O interactions to generate a 3-D network (figure 6).

Figure 3. View of the 2-D layer structure of **1**.Figure 4. ORTEP drawing (50% thermal) of **2**.Table 5. Hydrogen bonds in **2**.

D–H...A	d(D–H)	d(H...A)	d(D...A)	∠(DHA)
O3–H14...O1#1	0.85	1.91	2.76	172.09
O3–H6...O2#1	0.85	1.84	2.68	171.47
O3–H7...O5	0.85	1.96	2.80	169.10
O4–H8...O6#2	0.85	1.94	2.76	160.69
O4–H9...O7#3	0.85	1.90	2.75	177.03
O5–H10...O3#4	0.85	2.02	2.83	159.18
O5–H11...O6#2	0.85	1.96	2.77	157.90
O6–H13...O1#5	0.85	1.88	2.72	172.33
O6–H12...O1#6	0.85	1.90	2.72	162.43
O7–H15...O2	0.85	1.96	2.81	171.21
O7–H15...O5#5	0.85	1.79	2.83	165.70

Symmetry transformations used to generate equivalent atoms: #1: $x, y, z - 1$; #2: $x, y - 1, z$; #3: $x, y - 1, z - 1$; #4: $-x + 1, -y, -z$; #5: $-x + 1, -y + 1, -z + 1$; #6: $x, y + 1, z$.

Figure 5. View of the 1-D water tapes in **2**.Figure 6. View of the 3-D networks of **2** formed by hydrogen bonds; the benzotriazole rings were removed for clarity.

3.3. Description of the crystal structure for $[Mn(btaa)_2(H_2O)_2]_n$ (**3**)

The compound possesses a lamellar structure similar to that of $[Mn(4-cba)_2(H_2O)_2]_n$ [26]. As shown in figure 7, Mn1 sits at a crystallographic inversion center and has an octahedral coordination geometry, with equatorial positions defined by four oxygens from four symmetry-related carboxylates of btaa with Mn–O lengths of 2.150(2) and 2.173(2) Å, and two axial positions by two symmetry-related waters with Mn–O length of 2.203(2) Å. Each btaa links two Mn(II)s through carboxylate in a *syn-skew* coordination [mode (c) in scheme 1], and each Mn(II) connects four btaa ligands along the [0 1 0] and [0 0 1] directions to form a 2-D grid-like open-framework, in which Mn(II)s are arranged in an ideal layer and btaa lie on the two sides of the layer. The 2-D layered structure of **3** presents a (4, 4) topology when the Mn(II) is regarded as

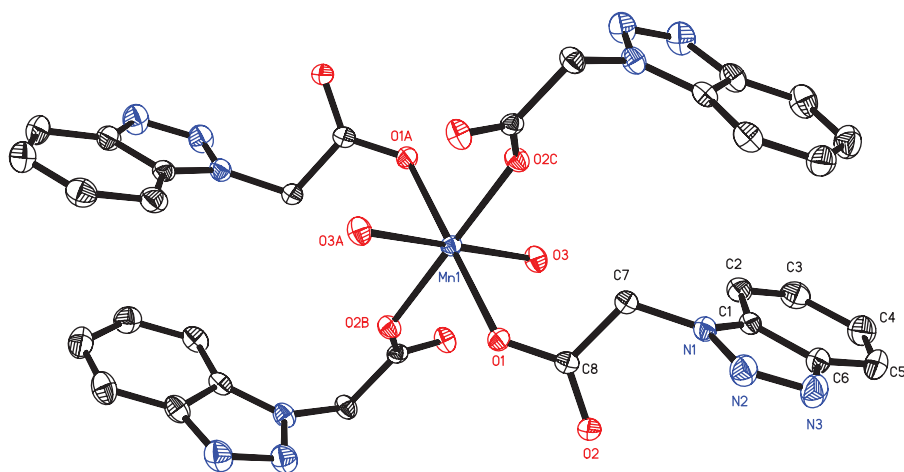


Figure 7. ORTEP drawing (50% thermal) of **3**.

connected node and the carboxylate of btaa as linker (figure 8). The nearest Mn(II)⋯Mn(II) distance is 5.302(3) Å through carboxylate.

Hydrogen bonds originating from the coordinated water, coordinated carboxylate oxygen, and nitrogen of triazole group ($O3 \cdots O1A = 2.756$ Å and $O3 \cdots N2B = 2.890$ Å, and the angles $O3-H8 \cdots O1A = 158.89^\circ$, $O3-H9 \cdots N2B = 162.81^\circ$; symmetry code a: $-x + 2, y + 1/2, -z + 3/2$; b: $x, 1 + y, z$) play an important role in the stabilization of the layer structure.

The btaa ligands adopt different coordination modes in the three complexes; chelated tridentate in **1**, terminal monodentate mode in **2**, and *syn-skew* bidentate in **3**, suggesting a flexible coordination capability of btaa. The influence of secondary ligands on the molecular assembly is also apparent. In **1**, bipy restricts the formation of higher dimensional framework. In **2**, the carboxylate is deprotonated, but interlinked by strong O-H⋯O hydrogen bonds with the crystal-lattice water molecules, so only a mononuclear compound is formed. In **3**, H₂O makes the construction of a 2-D network possible.

3.4. IR spectrum and thermal stability analysis

The absence of strong bands around 1700 cm⁻¹ in the IR spectra of **1–3** indicates that 1H-benzotriazole-1-acetic acid is completely deprotonated as btaa anions. The difference, Δ value, between the asymmetric and symmetric stretching frequencies [$\gamma_{as}(\text{COO})$ and $\gamma_s(\text{COO})$] reflects coordination of carboxylate [27]. The peaks at 1603 and 1567 cm⁻¹ for **1**, 1603 cm⁻¹ for **2**, and 1608 cm⁻¹ for **3** are attributed to $\gamma_{as}(\text{COO})$, while those at 1398 cm⁻¹ for **1**, 1393 cm⁻¹ for **2**, and 1444 cm⁻¹ for **3** are ascribed to $\gamma_s(\text{COO})$. The Δ values of 205 and 169 cm⁻¹ for **1** and 164 cm⁻¹ for **3** are indicative of bidentate chelated or bridging coordination. The Δ value of 210 cm⁻¹ for **2** is possibly due to the existence of strong hydrogen bonds between the uncoordinated carboxylate oxygen and water. These conclusions are also supported by X-ray diffraction measurements.

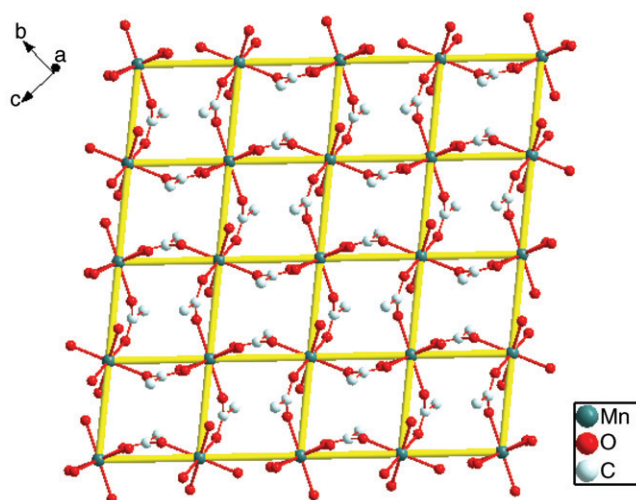


Figure 8. View of the 2-D grid-like framework of **3**; the benzotriazole rings were removed for clarity.

TGA for **1–3** were performed under a flow of N_2 gas (figure S1). For **1**, the TG curve shows three main steps of weight loss. The first step was started at $50^\circ C$ and completed at $80^\circ C$, corresponding to the release of one crystal-lattice water. The observed weight loss of 3.52% is close to the calculated value (3.45%). The weight loss of 71.28% during the second and third steps from $224^\circ C$ to $452^\circ C$ corresponds to the release of 2,2'-bipy, acetate and btaa (Calcd 71.94%), giving CdO as the final decomposition product which constitute 25.20% (Calcd 24.61%). For **2**, the weight loss of 30.02% during the first and second steps from $58^\circ C$ to $206^\circ C$ corresponds to the loss of six crystal-lattice water and four coordination water molecules (Calcd 30.62%). The third-step weight loss of 57.19% (Calcd 56.75%) from $258^\circ C$ to $390^\circ C$ corresponds to the decomposition of btaa. Assuming the residue is NiO, the observed weight (12.79%) is in agreement with the calculated value (12.63%). Compound **3** loses coordination water in the range $170\text{--}205^\circ C$ with a weight loss of 8.36% (Calcd 8.12%). The btaa ligands are released from $300^\circ C$ to $365^\circ C$ with a weight loss of 76.02% (Calcd 75.88%), giving MnO as the final decomposition product at 15.62% (Calcd 16.00%).

3.5. Photoluminescence

Metal–organic polymeric complexes with a d^{10} closed-shell electron configuration exhibit fluorescent properties [28, 29]. Here, the fluorescence of **1** in the solid state at room temperature was examined (figure 9). Complex **1** exhibits pure blue photoluminescence with an emission maximum at *ca* 424 nm upon excitation at 355 nm, while free Hbtaa displays weak fluorescence emission with a maximum at 356 nm upon excitation at 325 nm in solid state, and 2,2'-bipy displays one weak emission band at *ca* 530 nm [30]. The photoluminescent intensity of **1** is much stronger than those of the free ligands, indicating that the photoluminescence mechanism of **1** is significantly different from those of both ligands. The luminescence band at *ca* 424 nm of **1** may be

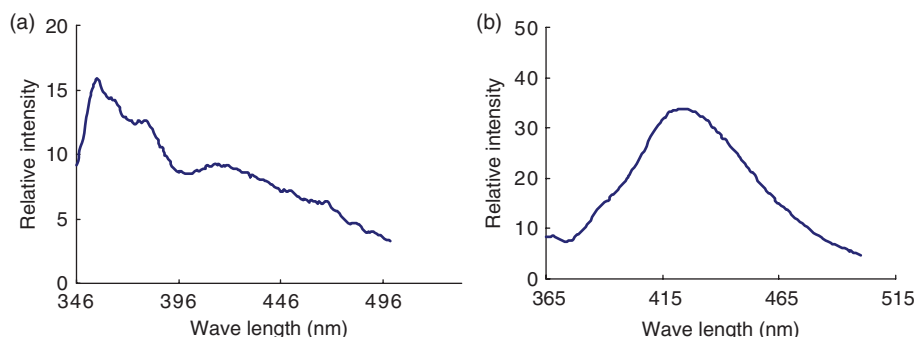


Figure 9. Emission spectra of (a) Hbtaa ligand and (b) **1** in the solid state at room temperature.

assigned to $\pi \rightarrow 5s$ ligand-to-metal charge transfer (LMCT) [24, 31], and the enhanced luminescence intensity in **1** may be attributed to the conformational restriction of the ligands due to its coordination with the metal ion and thus reducing the loss of energy through a radiationless pathway [32].

4. Conclusion

The syntheses and crystal structures of three new complexes containing 1H-benzotriazole-1-acetic acid ligand are reported. Different coordination modes of btaa and secondary ligands exert influences on the final molecular assembly: **1** with a 1-D chain structure, **2** with an isolated mononuclear structure, and **3** displaying a 2-D grid-like framework. Hydrogen bonds and π - π stacking interactions play an important role in crystal packing and supramolecular frameworks. Complex **1** shows blue photoluminescence arising from LMCT.

Supplementary material

Crystallographic data (excluding structure factors) for the structure reported in this article have been deposited with the Cambridge Crystallographic Data Centre as supplementary publication No. CCDC – 736263, 736265, and 742510. The copies of the data can be obtained free of charge on application to CCDC, 12 Union Road, Cambridge CB21EZ, UK (Fax: (+44) 1223-336-033; E-mail: deposit@ccdc.cam.ac.uk). TG curves of **1–3** are shown in figure S1.

Acknowledgments

The authors gratefully acknowledge the Postgraduate Foundation of Taishan University (No. Y05-2-02).

References

- [1] O.R. Evans, W. Lin. *Acc. Chem. Res.*, **35**, 511 (2002).
- [2] R. Kitaura, K. Seki, G. Akiyama, S. Kitagawa. *Angew. Chem. Int. Ed. Engl.*, **42**, 428 (2003).
- [3] C.J. Kepert, T.J. Prior, M.J. Rosseinsky. *J. Am. Chem. Soc.*, **123**, 10001 (2001).
- [4] S. Noro, R. Kitaura, M. Kondo, S. Kitagawa, T. Ishii, H. Matsuzaka, M. Yamashita. *J. Am. Chem. Soc.*, **124**, 2568 (2002).
- [5] N.W. Ockwig, O. Delgado-Friedrichs, M. O'Keeffe, O.M. Yaghi. *Acc. Chem. Res.*, **38**, 176 (2005).
- [6] A.C. Sudik, A.R. Millward, N.W. Ockwig, A.P. Cote, J. Kim, O.M. Yaghi. *J. Am. Chem. Soc.*, **127**, 7110 (2005).
- [7] K. Inoue, H. Imai, P.S. Ghalsasi, K. Kikuchi, M. Ohba, H. Okawa, J.V. Yakhmi. *Angew. Chem. Int. Ed.*, **40**, 4242 (2001).
- [8] Y.L. Bai, J. Tao, R.B. Huang, L.S. Zheng. *Angew. Chem. Int. Ed.*, **47**, 5344 (2008).
- [9] K.Z. Shao, Y.H. Zhao, Y. Xing, Y.Q. Lan, X.L. Wang, Z.M. Su, R.S. Wang. *Cryst. Growth Des.*, **8**, 2986 (2008).
- [10] K.M. Buschbaum, Y. Mokaddem. *Eur. J. Inorg. Chem.*, 2000 (2006).
- [11] C.C. Stoumpos, E. Diamantopoulou, C.P. Raptopoulou, A. Terzis, S.P. Perlepes, N. Lalioti. *Inorg. Chim. Acta*, **361**, 3638 (2008).
- [12] X.M. Zhang, Z.M. Hao, W.X. Zhang, X.M. Chen. *Angew. Chem. Int. Ed.*, **46**, 3456 (2007).
- [13] J. Wang, M.H. Huang, P. Liu, W.D. Cheng. *J. Mol. Struct.*, **875**, 22 (2008).
- [14] C. Richardson, P.J. Steel. *Discuss. Faraday Soc.*, 992 (2003).
- [15] O.Z. Yesilel, A. Mutlu, O. Buyukgungor. *Polyhedron*, **28**, 437 (2009).
- [16] R. Murugavel, S. Kuppuswamy, A.N. Maity, M.P. Singh. *Inorg. Chem.*, **48**, 183 (2009).
- [17] T.L. Hu, W.P. Du, B.W. Hu, J.R. Li, X.H. Bu, R. Cao. *CrystEngComm*, **10**, 1037 (2008).
- [18] T. Huang, Q. Ye. *Acta Crystallogr., Sect. E*, **64**, m758 (2008).
- [19] Z.B. Zheng, R.T. Wu, J.K. Li, Y.F. Sun. *J. Mol. Struct.*, **928**, 78 (2009).
- [20] Z.B. Zheng, R.T. Wu, J.K. Li, Y.F. Sun. *J. Coord. Chem.*, **62**, 2324 (2009).
- [21] G.M. Sheldrick. *SHELXTL (Version 6.1)*, Bruker AXS Inc., Madison, WI, USA (2000).
- [22] Y.T. Wang, G.M. Tang, Y. Wu, X.Y. Qin, D.W. Qin. *J. Mol. Struct.*, **831**, 61 (2007).
- [23] R. Prajapati, L. Mishra, K. Kimura, P. Raghavaiah. *Polyhedron*, **28**, 600 (2009).
- [24] X.Z. Sun, Z.L. Huang, H.Z. Wang, B.H. Ye, X.M. Cheng. *Z. Anorg. Allg. Chem.*, **631**, 919 (2005).
- [25] L. Infantes, J. Chisholm, S. Motherwell. *CrystEngComm*, **5**, 480 (2003).
- [26] Y. Li, G.Q. Li, F.K. Zheng, J.P. Zou, W.Q. Zou, G.C. Guo, C.Z. Lu, J.S. Huang. *J. Mol. Struct.*, **842**, 38 (2007).
- [27] K. Nakamoto. *Infrared and Raman Spectra of Inorganic and Coordination Compounds*, 4th Edn, Wiley Press, New York (1986).
- [28] X. Shi, G. Zhu, X. Wang, G. Li, Q. Fang, X. Zhao, G. Wu, G. Tian, M. Xue, R. Wang, S. Qiu. *Cryst. Growth Des.*, **5**, 341 (2005).
- [29] X. Wang, C. Qin, E. Wang, Y. Li, N. Hao, C. Hu, L. Xu. *Inorg. Chem.*, **43**, 1850 (2004).
- [30] X. Shi, G. Zhu, Q. Fang, G. Wu, G. Tian, R. Wang, D. Zhang, M. Xue, S. Qiu. *Eur. J. Inorg. Chem.*, 185 (2004).
- [31] S.L. Zheng, J.H. Ying, X.L. Yu, X.M. Chen, W.T. Wang. *Inorg. Chem.*, **43**, 830 (2004).
- [32] B. Valeur. *Molecular Fluorescence: Principles and Applications*, Wiley-VCH, Weinheim (2002).